

## Classification of three-body quantum halos

A.S. JENSEN<sup>1</sup>, K. RIISAGER<sup>1</sup>, D.V. FEDOROV<sup>1</sup> and E. GARRIDO<sup>2</sup>

<sup>1</sup> *Institute of Physics and Astronomy, Aarhus University - DK-8000 Aarhus C, Denmark*

<sup>2</sup> *Instituto de Estructura de la Materia, CSIC - Serrano 123, E-28006 Madrid, Spain*

PACS. 21.45.+v – Few-body systems.

PACS. 03.65.Ge – Solutions of wave equations: bound states.

PACS. 21.80.+a – Hypernuclei.

**Abstract.** – The different kinds of behaviour of three-body systems in the weak binding limit are classified with specific attention to the transition from a true three-body system to an effective two-body system. For weakly bound Borromean systems approaching the limit of binding we show that the size-binding energy relation is an almost universal function of the three  $s$ -wave scattering lengths measured in units of a hyperradial scaling parameter defined as a mass weighted average of two-body equivalent square well radii. We explain why three-body halos follow this curve and why systems appearing above reveal two-body substructures. Three-body quantum halos 2-3 times larger than the limit set by zero hypermoment are possible.

*Introduction.* – Attempts for a general classification of halo states were started early in the development of the field, see e.g. [1], and have recently led to the suggested definition of halo states [2,3] as having more than 50% probability of being in a cluster configuration where more than 50% of this probability should be in a classically forbidden region. This definition is straightforward to apply for a two-body system, where one basically has to find the outer classical turning point in the radial motion. The three-body systems are more challenging [4] and it is the purpose of this paper to discuss their possible modes of behaviour.

One obvious point that needs clarification is how to generalize the outer classical turning point, that also can be used [2] to scale different halo systems so that e.g. nuclear and molecular halos can be compared in dimensionless units. For the interesting special case of Efimov states a universal scaling property predicting one Efimov state from the previous one has been developed, see [5, 6, 7]. Another point that has only been discussed briefly in the literature so far is how the transition from a three-body to a two-body state takes place as the binding potentials are changed [8]. Connected to this is the classification of possible three-body configurations into Borromean [9,10,11], tango [12] or other bound states. To clarify the principles we shall mainly consider systems where all particles are in relative  $s$ -waves, which dominate at large distances. Results of more realistic calculations will also be given for <sup>11</sup>Li and the hypertriton.

*Three-body systems.* – There is naturally more variability in three-body systems than in two-body systems. The three two-body subsystems might all play a role in the asymptotic region, so even in the weak-binding limit we should expect several types of behaviour to be possible, even for the simplest case of only relative  $s$ -waves. Systems with zero and one bound subsystem are called Borromean and tango systems, respectively.

In a two-body system the classical turning points are found by equating the total energy and the potential energy. In principle we can generalize this to three particles in a specified quantum state described by the wave function  $\Psi$  and find the probability for being in the non-classical region as  $\int |\Psi|^2 d\tau$ , where the integration is confined to regions with potential energy larger than the total energy. This will be much harder to calculate than for a two-body system and could therefore be a rather impractical condition. Furthermore, we are not assured that the wavefunction will behave in a simple way in the non-classical region; there might be configurations where one pair is in a forbidden region whereas the third particle is in an allowed region. We shall therefore here rather explore the possibility of generalizing the classical turning point into a three-body scaling radius and discuss two different types of “derivation” of it.

*First derivation.* – We use hyperspherical coordinates to describe the relative motion of three particles with masses  $m_i$ , where  $i = 1, 2, 3$ . The total mass is  $M = m_1 + m_2 + m_3$ , the individual momenta and coordinates are  $\mathbf{p}_i$  and  $\mathbf{r}_i$  and the hyperradius  $\rho$  is defined by

$$m\rho^2 \equiv \frac{1}{M} \sum_{i < k} m_i m_k (\mathbf{r}_i - \mathbf{r}_k)^2 = \sum_i m_i (\mathbf{r}_i - \mathbf{R})^2, \quad (1)$$

where  $\mathbf{R}$  is the center of mass coordinate and  $m$  is a mass unit chosen for convenience. The hyperradius is an average radius coordinate, applicable to all three-body systems and useful for all angular momenta and for non-spherical systems. The total mean square radius  $\langle r^2 \rangle$  is then via the particle sizes  $\langle r^2 \rangle_i$  given by

$$M \langle r^2 \rangle = m \langle \rho^2 \rangle + \sum_i m_i \langle r^2 \rangle_i. \quad (2)$$

It is natural to choose a three-body scaling radius  $\rho_0$  so that the arbitrary mass  $m$  enters in the same way in  $\rho$  and  $\rho_0$  and all measures of size, that typically rely on their ratio, become independent of  $m$ . The two-body scaling property relating size and binding energy can then be generalized if  $\langle \rho^2 / \rho_0^2 \rangle$  is an almost single-valued function of another dimensionless quantities  $Bm\rho_0^2/\hbar^2$ , where  $B$  is the three-body binding energy [8]. Such a scaling property is clearly an advantage when searching for a general definition of the scaling radius  $\rho_0$ . The relation should apply for systems consisting of particles with widely different masses and ranges of interactions. A tempting definition of  $\rho_0$  is to maintain the complete analogy to  $\rho$ , i.e.

$$m\rho_0^2 \equiv \frac{1}{M} \sum_{i < k} m_i m_k R_{ik}^2, \quad (3)$$

where  $R_{ik}$  is interpreted as the equivalent square well radius of the system consisting of particle  $i$  and  $k$ . As argued in [2] this definition is convenient in descriptions of three-body systems intermediate between two and three-body scaling.

*Hyperradial potential.* – The choice of hyperspherical coordinates leads to effective radial potentials obtained by adiabatic expansion or by averaging in other ways over the remaining set of angular coordinates. The classically allowed regions for such one-dimensional potentials are

easily defined. However, they could be completely different from the regions where the three pairs of particles are located in their classically allowed regions defined by the corresponding two-body potentials. In fact, it is entirely possible to have classical motion in the hyperradial coordinate while the system is in non-classical regions in real space. Hyperradial turning points are therefore useless as definitions of quantum halos and often without any resemblance to the length unit  $\rho_0$  defined above in terms of two-body properties.

It is instructive to consider the general behaviour of the hyperradial potential. For zero-range two-body potentials the only energy available through combination of parameters is  $\hbar^2/(2\mu\rho^2)$ , where  $\mu$  is a combination of reduced masses. With this large distance behaviour any number of solutions is possible, ranging from zero to the infinitely many Efimov states. For finite range interactions the ranges or alternatively the scattering lengths provide additional length parameters and the hyperradial potentials could approach zero faster than  $\rho^{-2}$ .

From [13] we obtain the large distance behaviour of the dominating lowest  $s$ -wave adiabatic potential as

$$V_{ad} = -\frac{\hbar^2}{2m\rho^2} \frac{16}{\pi} \sum_{i<k} \frac{a_{ik}}{\rho} \sqrt{\frac{\mu_{ik}}{m}} \equiv \frac{\hbar^2}{2m\rho^2} \frac{48}{\pi\sqrt{2}} \frac{a_{av}}{\rho}, \quad (4)$$

where the reduced mass is  $\mu_{ik} = m_i m_k / (m_i + m_k)$ , the  $s$ -wave scattering length is  $a_{ik}$  and the average scattering length is defined as

$$a_{av}\sqrt{m} \equiv \frac{\sqrt{2}}{3} \sum_{i<k} \sqrt{\mu_{ik}} a_{ik}. \quad (5)$$

The chosen normalization reduces  $a_{av}$  to the common  $a_{ik}$  when all three particles are identical. Thus the large distance behavior of  $V_{ad}$  in Eq.(4) is  $\rho^{-3}$  which is reached when  $\rho$  is comparable to  $48a_{av}/(\pi\sqrt{2})$ , see [13].

*Second derivation.* – Scaling can be shown analytically to occur for the special case of a  $K = 0$  wavefunction ( $K$  being the hypermoment) for square well two-body potentials of depth  $S_{ik}$  and radius  $R_{ik}$ . Here the effective hyperradial potential  $V$  can be obtained [8] as

$$V(\rho) = \frac{16}{3\pi} \sum_{i<k} \frac{S_{ik}}{\rho^3} \left( \sqrt{\frac{\mu_{ik}}{m}} R_{ik} \right)^3, \quad (6)$$

which is valid when  $\rho$  is several times larger than any of the square well radii. The square well two-body  $s$ -wave scattering length is given by  $a_{ik}/R_{ik} = -1 + \tan(K_{ik}R_{ik})/(K_{ik}R_{ik})$ , where  $K_{ik}$  is the zero energy wave number inside the square well, i.e  $\hbar^2 K_{ik}^2 / (2\mu_{ik}) = S_{ik}$ . Then  $K_{ik}^2 R_{ik}^2 = 2S_{ik}\mu_{ik}R_{ik}^2/\hbar^2$  is a specific function of  $a_{ik}/R_{ik}$ , which approaches the constant  $\pi^2/4$  when  $a_{ik}$  becomes much larger than  $R_{ik}$ . Thus the effective radial potential in Eq.(6) approaches the form

$$V(\rho) = \frac{\hbar^2}{2m\rho^2} \frac{4\pi}{3} \sum_{i<k} \frac{R_{ik}}{\rho} \sqrt{\frac{\mu_{ik}}{m}} \equiv \frac{\hbar^2}{2m\rho^2} \sqrt{8\pi} \frac{\rho_0}{\rho}, \quad (7)$$

where the definition of  $\rho_0$ ,

$$\rho_0\sqrt{m} \equiv \frac{\sqrt{2}}{3} \sum_{i<k} \sqrt{\mu_{ik}} R_{ik}, \quad (8)$$

reduces to that of Eq.(3) for identical masses and radii. Note that Eq.(8), in contrast to Eq.(3), employs a linear (not squared) summation. For systems where the two-body scattering lengths

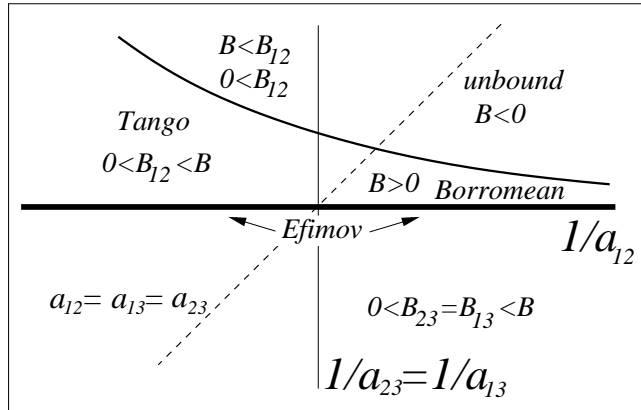


Fig. 1 – Sketch of the different regions of stability for a three-body system as functions of the inverse  $s$ -wave two-body scattering lengths  $a_{ik}$ . The central point corresponds to all  $a_{ik} = \infty$  which is assumed to be the threshold for binding of the first state in the  $i - k$  subsystem. All potentials are attractive or vanishing. Particles 1 and 2 are identical. The dashed line represents three identical particles. The two and three-body binding energies are  $B_{ik}$  and  $B$ , respectively.

are large, most of the wavefunction will reside in the region where Eq.(7) holds for  $K = 0$  and one clearly has scaling.

A desirable property of the scaling radius  $\rho_0$  would be that classically forbidden regions on average are given roughly by  $\rho > \rho_0$ . We can consider this question briefly for the specific  $K = 0$  solutions, where the probability  $P_{ik}$  for particles  $i$  and  $k$  being inside their square well radius  $R_{ik}$  for large  $\rho$  is

$$P_{ik}(\rho) = \frac{16}{3\pi} \left( \frac{R_{ik}}{\rho} \sqrt{\frac{\mu_{ik}}{m}} \right)^3. \quad (9)$$

This probability is  $1/2$  for  $\rho = 2(4/(3\pi))^{1/3} \sqrt{\mu_{ik}/m} R_{ik}$  which indicates that systems reside mainly in classically forbidden regions if their mean square radii are somewhat larger than  $\rho_0^2$ .

We do not believe that the  $K = 0$  wave functions are realistic solutions for the weakly bound systems since they do not allow for any form of correlations between the particles. For very loosely bound systems where  $a_{av}$  is much larger than  $\rho_0$  the potential will fall off as  $\rho^{-2}$  between  $\rho_0$  and  $a_{av}$ , i.e. slower than  $\rho^{-3}$  as for a pure  $K = 0$  solution.

*Scaling properties.* – The scaling radius will be used to look for scaling properties of three-body systems in the weak binding limit. We are aiming for as universal properties as possible, but the rather different types of structure that occur in three-body systems means we first have to look at how they can be classified. In fig.1 we illustrate the various stability regions as function of scattering lengths. At the border between tango and Borromean regions one subsystem has a bound state with zero energy. On the thick horizontal line two identical subsystems have bound states of zero energy and the infinitely many Efimov states arise.

The figure only shows the region where  $a_{23} = a_{13}$ , appropriate e.g. when particles 1 and 2 are identical, but already indicates that two distinct types of transitions can occur as a function of  $a_{12}$ , namely moving from the tango region (the 23 and 13 subsystems are unbound) from left to right either directly into unbound systems or through the Borromean region. To see this in detail we now turn to the numerical results and show in fig. 2 the region of weak binding for a number of both schematic and realistic examples. Through Eq.(2) this scaling

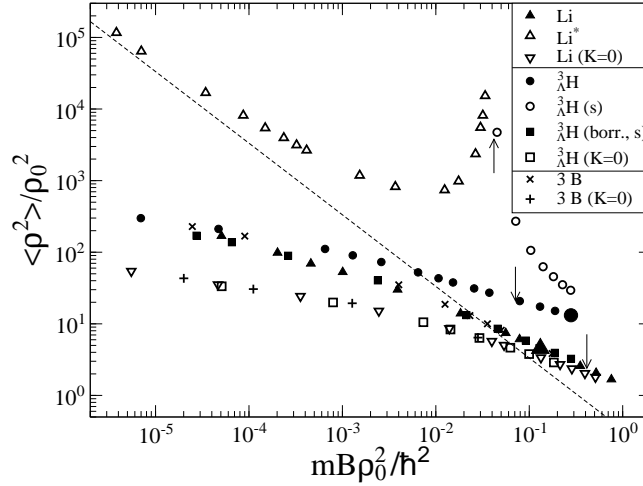


Fig. 2 – Scaling plot for three-body halos. The ratio of the halo and effective potential mean square radii is plotted versus the scaled separation energy. The definition of scaling radius in Eq.(8) is used. The dashed line represents the Efimov states for minimum attraction. Triangles are for masses corresponding to  ${}^{11}\text{Li}$ . Squares and circles are for  ${}^3_\Lambda\text{H}$ . The realistic points are indicated by a large closed triangle and square, respectively. The stars and crosses refer to a system of three different particles with two fixed scattering lengths while the third is varied. Almost indistinguishable curves arise for three identical Borromean bosons by varying the common scattering length. The arrows indicate transitions from (i) Borromean to tango region (closed circles), (ii) tango directly to unbound three-body system (open circles), (iii) Borromean to either two bound subsystems or the tango region (stars, crosses, open and closed triangles and squares) all occurring approximately at the same point. The excited states of  ${}^{11}\text{Li}$  all correspond to a bound  $n\text{-}^9\text{Li}$  system.

plot displays the mean square radius of the system in units of  $\rho_0^2$  versus the dimensionless binding energy  $mB\rho_0^2/\hbar^2$  [2], where  $B$  is the three-body binding energy. Zero binding energy corresponds to three non-interacting particles at rest.

We shall in this letter use the scaling radius defined in Eq.(8), where  $R_{ik}$  is the radius of the square well with the same scattering length and effective range as the actual two-body potential. Changing to the other definition in Eq.(3) has essentially no effect on the hypertriton examples, whereas the different  ${}^{11}\text{Li}$  points move by about 30%. The resulting figure is practically indistinguishable from the present one, except that the perfect scaling for  $K=0$  is violated slightly. There is no strong preference for any of these two definitions of  $\rho_0$ .

The first analysis in [8] assumed that simple systems at least asymptotically would correspond to a single value of the hypermoment  $K$ . We have artificially restricted the wavefunctions for different systems to contain only  $K=0$  terms and find that these systems, as argued above, indeed do scale and lie on a single curve. However, the points corresponding to more realistic calculations lie above this  $K=0$  curve and can be grouped and understood as follows.

In the realistic  ${}^3_\Lambda\text{H}$ -structure the neutron and proton are almost in a deuteron configuration (close circles) whereas the  $\Lambda$ -particle is far outside but still bound by about 0.14 MeV. Thus this is a tango system and the large size is almost entirely due to the  $\Lambda$ -deuteron extension, i.e. of two-body character. By using a simplified form for the neutron-proton interaction with only  $s$ -waves the position is slightly higher than the realistic point. By decreasing this neutron-proton attraction the binding decreases moderately while the radius drastically increases (open circles). This off hand surprising property can be understood from fig. 1 by

moving horizontally from the tango region to the right, increasing  $1/a_{12}$ . For sufficiently weak initial binding, i.e. large values of  $1/a_{13}$ , the threshold for  $\Lambda$ -deuteron binding is reached instead of the Borromean region as we decrease the attraction of the only bound subsystem. Thus the diverging radius is due to  $\Lambda$ -deuteron two-body threshold and not related to the neutron-proton threshold.

Decreasing the  $s$ -wave attraction between neutron and proton while maintaining all other parts of the realistic interaction (filled circles), now leads from tango into the Borromean region of fig.1, i.e. the three-body system remains bound even after the neutron-proton potential is too weak to form a bound two-body state. The result is a completely different curve in fig. 2 much more in agreement with the logarithmic divergence expected from [8], although still significantly above the  $K = 0$  curve. We stress that nothing drastically happens at the arrow where the deuteron becomes unbound (scaled binding energy about 0.08).

The realistic point for the Borromean nucleus  ${}^{11}\text{Li}$  is at a scaled binding energy of 0.13 in fig. 2. By decreasing the  $s$ -wave attraction in the neutron- ${}^9\text{Li}$  systems, i.e. going vertically upwards in fig. 1 approaching the threshold, the binding decreases and the radius increases corresponding to a logarithmically diverging curve in fig. 2 (filled triangles) eventually approaching that of the Borromean hypertriton example. A similar behaviour is seen for a hypothetical hypertriton with only  $s$ -waves included (filled squares) but with a slightly increased nucleon- $\Lambda$  attraction. Then we move horizontally from the tango to the Borromean region. For a Borromean system of three particles (stars) where the three masses and scattering lengths are equal or differ substantially, we again follow the same trajectory by changing one scattering length.

By increasing the  $s$ -wave attraction in the neutron- ${}^9\text{Li}$  systems, i.e. vertically approaching the Efimov limit in fig. 1, larger binding and smaller radius result as expected. The resulting non-Borromean  ${}^{11}\text{Li}$  ground state resembles more and more an ordinary nuclear state. However, at some point an excited state appears, i.e. the first Efimov state (open triangles). At first it is very weakly bound and close to the Efimov line. As the attraction and the three-body binding energy increases the size at first decrease and then “turn around” and increase again as the binding energy of the two bound two-body subsystems approach and finally overtake the three-body binding energy [5]. As the two-body threshold is approached the third excited state (second Efimov state) should appear on the dashed line. Unfortunately the mass ratio (neutron to  ${}^9\text{Li}$ ) is relatively small and the next state is many orders of magnitude outside the scale of the plot, i.e. outside the reach of experimental as well as most numerical techniques.

One remaining question is the approach of the two sets of points, related to hypertriton and  ${}^{11}\text{Li}$ , at very small binding energy. Both these sets arise by approach of (different) thresholds for Borromean binding in fig. 1. When the majority of the radial wave function is located in the tail of the adiabatic potential in Eq.(4) then  $a_{av}$  is a decisive length parameter. One could then erroneously be led to conclude that  $a_{av}$  determines the size-binding relations and the threshold for Borromean binding in fig. 1. However, the absolute scale of the energy can not be determined from one parameter alone, the short distance behaviour is also indispensably necessary [6, 7, 14].

To understand this we imagine that we reduce the ranges of the potentials while increasing the strengths to maintain the scattering lengths. This zero-range limit results in the Thomas collapse and infinitely many bound states at small distances [14]. To avoid this unphysical behaviour some kind of renormalization is needed. The simplest is to maintain the large distance behavior while only using the two-body potentials down to a distance below which the structure is uninteresting. The two-body results can then be expressed in units of such a rather arbitrary length parameter. The effect on a three-body system can then be anticipated mimicked by a similar renormalization by use of a hyperspherical length unit. However, this

is precisely the content of fig. 2 where we used  $\rho_0$  as the scale parameter.

The curves in fig. 2 coinciding at small binding are therefore an almost universal curve as indicated by the convergence in the figure. It would perhaps be rather fortuitous if this simple renormalization procedure in hyperradius results in a universal rescaled curve. The average scattering lengths for the four cases in the weak binding limit vary from 4 fm to 20 fm whereas the ratio  $a_{av}/\rho_0$  varies between 1.7 and 4.2. However,  $a_{av}$  only determines the adiabatic potential for distances smaller than the scattering lengths and larger than the potential ranges. These conditions are not well fulfilled for the examples in fig. 2. Thus constant  $a_{av}/\rho_0$  should not necessarily arise, since  $a_{av}$  should be replaced by a complicated function of all three  $a_{ik}$ . This is not contradicting the numerical results in fig. 2 which is obtained without use of  $a_{av}$ . Thus the emerging numerical curve is almost universal providing rather well defined scaling properties.

*Summary and conclusion.* – Three-body quantum halos were previously believed to appear along the  $K = 0$  curve [8]. This conclusion was reached by omitting constant terms compared to the leading order logarithmically diverging term. However, the present more refined analysis reveals the correct higher lying universal curve approached in the weak binding limit. In fact asymptotically these curves differ by a constant factor. In any case three-body quantum halos can appear above the  $K = 0$  curve, i.e. allowed in a larger window and being a factor of 2–3 larger than expected. One implication is that  $K = 0$  wavefunctions cannot be used in the weak binding limit due to the coherent large-distance contributions from more than one subsystem. For stronger binding a  $K = 0$  basis is simply incomplete.

In fig. 1 ground state three-body halos appear just below the line separating the Borromean from the unbound region. On top of this the Efimov effect can also give “super-halos” in excited states. Ground state two-body halos can appear just below the line separating the tango from the unbound region. In fig. 2, three-body halos where the three-body dynamics dominate will appear on or below the (almost) universal curve. All systems falling above are influenced by an effective two-body threshold and correspond either to the Efimov line (caused by the threshold in two subsystems) or the tango-unbound line in fig. 1. We stress that all quantities used to place a system in fig. 2 in principle can be measured experimentally and that our results therefore can be used to classify the three-body nature of realistic systems.

## REFERENCES

- [1] RIISAGER K., *Rev. Mod. Phys.*, **66** (1994) 1105.
- [2] RIISAGER K., FEDOROV D.V. and JENSEN A.S., *Europhysics Lett.*, **49** (2000) 547.
- [3] JENSEN A.S. and RIISAGER K., *Phys. Lett. B*, **480** (2000) 39.
- [4] NIELSEN E., FEDOROV D.V., JENSEN A.S. and GARRIDO E., *Phys. Rep.*, **347** (2001) 373.
- [5] EFIMOV V., *Phys. Lett. B*, **33** (1970) 563.
- [6] AMORIM A.E.A., FREDERICO T. and TOMIO L., *Phys. Rev. C*, **56** (1997) R2378.
- [7] FREDERICO T., TOMIO L., DELFINO A. and AMORIM A.E.A., *Phys. Rev. A*, **60** (1999) R9.
- [8] FEDOROV D.V., JENSEN A.S. and RIISAGER K., *Phys. Rev. C*, **49** (1994) 201; **50** (1994) 2372.
- [9] ZHUKOV M.V., DANILIN B.V., FEDOROV D.V., BANG J.M., THOMPSON I.J. and VAAGEN J., *Phys. Rep.*, **231** (1993) 151.
- [10] GOY J., RICHARD J.-M. and FLECK S., *Phys. Rev. A*, **52** (1995) 3511.
- [11] MOSZKOWSKI S., FLECK S., KRIKEB A., THEUSSL L., RICHARD J.-M. and VARGA K., *Phys. Rev. A*, **62** (2000) 032504.
- [12] ROBICHEAUX F., *Phys. Rev. A*, **60** (1999) 1706.
- [13] JENSEN A.S., GARRIDO E. and FEDOROV D.V., *Few-Body Systems*, **22** (1997) 193.
- [14] FEDOROV D.V. and JENSEN A.S., *J. Phys. A*, **34** (2001) 6003.